Removal of Perylene from Water Using Block Copolymer Nanospheres or Micelles

FRED HENSELWOOD, GUOCHANG WANG, GUOJUN LIU

Department of Chemistry, The University of Calgary, 2500 University Drive, NW, Calgary, Alberta, Canada T2N 1N4

Received 21 January 1998; received 25 March 1998

ABSTRACT: Water-soluble nanospheres with poly(acrylic acid) (PAA) coronas were prepared from poly(2-cinnamoylethyl methacrylate)-*block*-PAA (PCEMA-*b*-PAA) and P(CEMA-*ran*-OEMA)-*b*-PAA, where "*ran*" denotes the random incorporation of 2-octanoylethyl methacrylate (OEMA) into the PCEMA block. These nanospheres and polystyrene-*block*-PAA micelles uptake perylene, a polycyclic aromatic hydrocarbon (PAH), from water. The nanospheres or micelles, with the sorbed perylene, are precipitated by $CaCl_2$. These nanospheres may be useful in concentrating PAHs present in trace amounts in water for chemical analysis or in the reclamation of water contaminated by PAHs. Investigated in this article are factors that govern the capacities of the nanospheres and micelles, and the critical calcium concentration for inducing nanosphere or micelle precipitation. © 1998 John Wiley & Sons, Inc. J Appl Polym Sci 70: 397–408, 1998

Key words: nanospheres; water reclamation; block copolymer; micelles

INTRODUCTION

Due to their potential use in controlled drug release, water-soluble block copolymer micelles have attracted much attention recently.[1–8] In a previous article in this series,[9] we reported the preparation of water-soluble "permanent micelles" or "nanospheres" from poly(2-cinnamoylethyl methacrylate)-*block*-poly(acrylic acid) (PCEMA-*b*-PAA) by photocrosslinking the PCEMA cores of the diblock micelles:

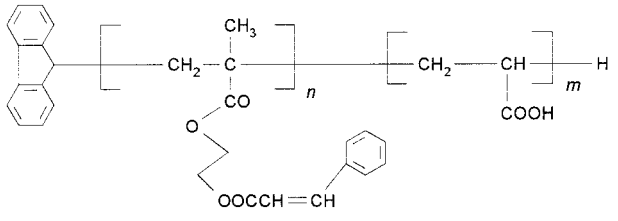

Correspondence to: G. Liu.

Journal of Applied Polymer Science, Vol. 70, 397–408 (1998)
 CCC 0021-8995/98/020397-12

The water-stable nanospheres sorbed organic compounds, such as perylene from water with a high partition coefficient.[10] The nanospheres with the sorbed perylene could then be precipitated by divalent cations, such as Ca^{2+} and Ba^{2+}. Based on these results, we proposed the use of the nanospheres in concentrating organic compounds present in trace amounts in water for chemical analysis or in the reclamation of water contaminated by organic compounds such as polycyclic aromatic hydrocarbons (PAHs).

In this article, we examine how various factors affect the capacities of these nanospheres in uptaking perylene and the critical calcium concentration, $[Ca^{2+}]^*$, above which the nanospheres precipitate from water. In the water reclamation application, the nanospheres may be added to a water reservoir in the open to extract organic compounds. The exposure of the nanospheres to sunlight may cause further CEMA crosslinking. Highly crosslinked nanospheres may not function effectively as "traps" for organic compounds, be-

Table I Characteristics of the Diblocks Used

Polymer	n/m from NMR	x from NMR	$\bar{M}_w$ from GPC	$\bar{M}_w/\bar{M}_n$ from GPC	dn_r/dc (mL · g^{-1})	$10^{-5}\bar{M}_w$ (g · mol^{-1})	$10^{-2}n$	$10^{-2}m$
Polymer 1 in *t*BA form[a]	2.5		6.0×10^4	1.09	0.136	1.47	4.7	1.91
Polymer 1 in AA form[b]		100%			0.143	1.31	4.5	1.84
Polymer 2 in *t*BA form[a]	0.65	100%	6.9×10^4	1.07	0.111	1.66	3.6	5.6
Polymer 3		91%						
Polymer 4		70%						
PS-*b*-PAA[c]	0.092						0.34	3.7

[a] NMR measurements were performed in deuterated chloroform and light scattering in methylene chloride. GPC was done in tetrahydrofuran.
[b] Light scattering experiment was performed in DMF.
[c] Characterization data of this polymer were supplied by Polymer Source, Inc. The symbols n and m denote the number of styrene and CEMA units in the diblock, respectively.

cause both the organic compound uptake rate and capacity of the nanospheres may decrease with increased CEMA crosslinking. To eliminate this potential problem, we replaced some of CEMA units of the PCEMA block with non-crosslinkable octanoylethyl methacrylate (OEMA) units to produce P(CEMA-*ran*-OEMA)-*b*-PAA, where *ran* denotes the "random" incorporation of OEMA into the PCEMA block at a molar fraction of $1 - x$.

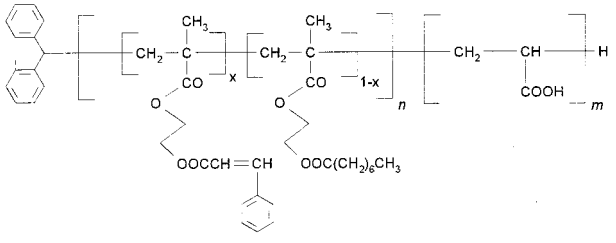

How the change in the nanosphere core structure affects their performances as potential traps for perylene, one PAH, is also investigated. The effect of crosslinking on the performances of the nanospheres is examined by comparing their performances with that of polystyrene-*block*-poly(acrylic acid) (PS-*b*-PAA) micelles and PCEMA-*b*-PAA micelles.

EXPERIMENTAL

Polymer Synthesis and Characterization

The precursors to PCEMA-*b*-PAA and P(CEMA-*ran*-OEMA)-*b*-PAA were poly(2-hydroxylethyl methacrylate)-*block*-poly(*t*-butyl acrylate) (PHEMA-*b*-P*t*BA). PHEMA-*b*-P*t*BA with the hydroxyl groups protected by trimethylsilyl was synthesized by anionic polymerization as described previously.[9,11] To prepare P(CEMA-*ran*-OEMA)-*b*-PAA, PHEMA-*b*-P*t*BA, ~ 5 wt % in pyridine, was reacted with freshly distilled octanoyl chloride (Aldrich, 99%) for 2 h at 21°C and then with 1.5 times excess of cinnamoyl chloride (Aldrich, 98%) for an additional 16 h. The polymer was precipitated into water, dissolved in tetrahydrofuran, and precipitated into a methanol/water mixture (v/v, 3/1). The *t*-butyl group of the P*t*BA block was cleaved following a method described previously.[11–13] The synthesis of PCEMA-*b*-PAA is similar to that of P(CEMA-*ran*-OEMA)-*b*-PAA, except the use of octanoyl chloride.

A total of two PHEMA-*b*-P*t*BA samples were used in this study. After cinnamation and *t*-butyl group removal, the corresponding PCEMA-*b*-PAA samples are polymers 1 and 2, respectively (Table I). Polymer 1 has a relatively short PAA block and is not directly soluble in water, and polymer 2 is soluble in warm water. Polymers 1 and 2 and their precursors were characterized by NMR, light scattering, and gel permeation chromatography (GPC) following procedures described previously.[9] The GPC system was calibrated with polystyrene standards.

Polymers 3 and 4, P(CEMA-*ran*-OEMA)-*b*-PAA with different contents of OEMA, were derivat-

ized from the PHEMA-*b*-P*t*BA precursor to polymer 2. Polymer 4 has a higher OEMA content than polymer 3.

Nanosphere Preparation and Characterization

Nanospheres 1–4 were prepared from polymers 1–4, respectively. Polymer 1 micelles were prepared in DMF/water with 20%, by volume, of DMF[9] and polymer 2–4 micelles were prepared in water at ~ 65°C. Nanospheres were obtained by irradiating the micelles with light from a 500-W mercury lamp filtered through a 260-nm cut-off filter.

Transmission electron microscopy (TEM) and dynamic light scattering were used to characterize the nanospheres. TEM specimens were prepared by aspirating a fine spray of an aqueous nanosphere solution using a home-built device[14] onto a Formvar-coated copper grid. The samples were stained by OsO_4 and viewed with a Hitachi-7000 electron microscope operated at 100 kV. For dynamic light scattering measurements, the nanospheres were dissolved in dimethylsulfoxide (DMSO) and centrifuged at 4,500 rpm for half an hour to remove dust.

PS-*b*-PAA Micelles

PS-*b*-PAA (Polymer Source, Inc.) micelles were prepared by refluxing the polymer in water for 24 h. For TEM study, the micelles were sprayed on Formvar-coated copper grids. The grids were then immersed in a uranyl acetate solution, ~ 10 $mg \cdot mL^{-1}$, in water/methanol containing 80% methanol by volume for 1 h before they were rinsed in water.

Preparation of Aqueous Perylene Solution

Solid perylene was sonicated in 250 mL of water for $\frac{1}{2}$ h. The mixture was then allowed to settle over a 3-day period. After centrifuging at 4.5 $\times 10^3$ rpm for $\frac{1}{2}$ h, the solid particles were removed by filtration once through filter paper and once through two nylon filters (pore size $\times$ 0.45 μm, Chromatography Specialties) connected in series. The filtrate was diluted to a final volume of 300 mL. The solution was homogeneous, because the fluorescence intensities of the samples taken from the top and bottom of the container were the same. By comparing the fluorescence intensity of this sample with that of a sample at $2.0 \times 10^{-8}M$, prepared by adding a known amount of a perylene solution in acetone into water (final acetone volume was <0.1%), we obtained a perylene concentration of $1.9 \times 10^{-8}M$ for the aqueous sample. Despite the homogeneity of the solution at the time of use, the solution turned out to be colloidal, because some perylene precipitated in 1 year.

Nanosphere Solution

Nanosphere 1, 25.0 mg, was dissolved by heating in 5.0 mL of DMSO at 80°C overnight. After cooling, 10 mL of water was added. The solution mixture was then transported into a dialysis tube (Spectrum Medical Industries, Inc.) and dialyzed in a 1000 mL beaker against distilled water for 3 days. The distilled water was replenished constantly by leaving a small stream running. The dialyzed solution was then transferred to a volumetric flask and diluted to a final volume of 50.0 mL. Solutions of nanosphere 2–4 were prepared in water directly.

Fluorescence Measurements

All fluorescence measurements were conducted on a Photon Technology International Alpha Scan system equipped with a 75-W xenon lamp. Spectra were reported as they were recorded without correcting for wavelength-dependent lamp emission efficiency and photomultiplier tube response. For following the kinetics of perylene insertion into nanosphere or micelle cores, a bandpass filter with a transmission efficiency of 18% at 410 nm was used on the excitation side.

Perylene Uptake Kinetics

After mixing 1.00 mL of a nanosphere solution with 2.00 mL of the aqueous perylene solution, the fluorescence intensity change at 475 nm was continuously monitored for 10–12 h with the excitation wavelength fixed at 410 nm.

Nanosphere Capacity Measurement

The capacity of the nanospheres refers to the maximum amount of perylene uptake per unit weight of polymer. We followed the method of Nawakowska and colleagues[15] for evaluating the capacity of nanospheres 2–4 and PS-*b*-PAA micelles for perylene sorption. The capacity of nanosphere 1 was not determined, because the nanospheres were stable in water only for days instead

of weeks. The reduced stability was due to the relatively thin PAA shell in nanosphere 1.

Different volumes of a perylene solution in acetone, 2.10 mg · L^{-1}, were added to clean sample vials. The acetone was evaporated and to each vial was added 4.00 mL of a nanosphere solution at ~ 0.07 mg · mL^{-1}. The vials were subsequently capped, wrapped in aluminum foil, and stirred for 3 weeks. Perylene fluorescence intensity was measured after the samples were centrifuged at 1,500 rpm for 10 min to remove perylene particles not solubilized.

Nanosphere Precipitation

A perylene-saturated aqueous nanosphere solution was centrifuged and the supernatant was taken. To it were added different volumes of a 0.100*M* $CaCl_2$ solution in 10-μL intervals. After each addition, the sample was stirred for 2 min, centrifuged for 10 min, and measured for its fluorescence intensity.

RESULTS AND DISCUSSION

Polymer Properties

NMR was used to determine the CEMA-to-acrylic acid (AA) molar ratios, n/m, for polymers 1 and 2 and the CEMA molar fraction, x, in the hydrophobic block for polymers 3 and 4 (Table I). Shown in Figure 1 is the ^{1}H NMR spectrum of polymer 4 with all the peaks assigned. The OEMA content for this sample is 30% or x is 70%. Although not confirmed, we expect the OEMA to be randomly distributed in the PCEMA block.

Also shown in Table I are the weight-average molar masses, $\bar{M}_w$, and polydispersity indices, $\bar{M}_w/\bar{M}_n$, for polymers 1 and 2. Because the GPC instrument was calibrated with polystyrene standards, the $\bar{M}_w$ values determined from GPC are not true. Thus, light scattering $\bar{M}_w$ were used to calculate n and m, the number of CEMA and AA repeat units in different diblocks. The dn_r/dc values in Table I are the measured specific refractive index increments of the polymers in the different solvents used for light scattering studies.

PS-*b*-PAA was purchased from Polymer Source, Inc. It was shown to have a low polydispersity. The numbers of styrene and AA units, n and m, were calculated from monomer to initiator feeding ratios.

Nanosphere and Micelle Properties

Properties of the nanospheres and the PS-*b*-PAA micelles are summarized in Table II. The CEMA double bond conversion ranged from 15 to 35%. The nanospheres all had narrow size distributions. This is seen from the TEM image of nanosphere 4 shown in Figure 2. The hydrodynamic radius of the nanospheres, R_h, increased with OEMA content. Other than nanosphere 1, static light scattering was not used to obtain the nanosphere weight-average molar mass, $\bar{M}_w$, and radius of gyration, R_G.

Illustrated in Figure 3 is a TEM image of PS-*b*-PAA micelles. The micelle shells look darker and the cores lighter because uranyl acetate selectively stained the PAA block. The large holes in the image were formed due to the local breaking down of the substrate Formvar film in methanol/water. The micellar particles have an average diameter of ~ 35 nm. The hydrodynamic radius of the micelles determined in a 0.100*M* HCl aqueous solution at the scattering angle of 150° was 41 nm.

Fluorescence Spectra of Perylene

Illustrated in Figure 4 is a fluorescence spectrum of perylene of a perylene-nanosphere solution. This solution was prepared by mixing and equilibrating 2.00 mL of the aqueous perylene solution with 1.00 mL of a nanosphere solution at 6.27 $\times$ 10^{-5} mg · mL^{-1} for 2 days. The perylene spectrum was obtained by subtracting that of a sample containing nanospheres only from that of the perylene-nanosphere solution mixture.

Capacity Determination

Plotted in Figure 5 is the variation in perylene fluorescence intensity as a function of the amount of perylene equilibrated with 4.00 mL of a nanosphere 3 and a PS-*b*-PAA micellar solution at the nanosphere and micellar concentrations of 8.6 $\times$ 10^{-2} and 0.236 mg · mL^{-1}, respectively. The fluorescence intensity increased sharply initially with the perylene amount, m_{Pe}, and then leveled off.

The initial fluorescence intensity increase with increasing perylene amount is expected due to their solubilization into the nanosphere or micelle cores. The leveling off of the fluorescence intensity at high perylene contents is reasonable as well. The nanospheres and micelles have only a certain capacity. Once saturated, they cannot up-

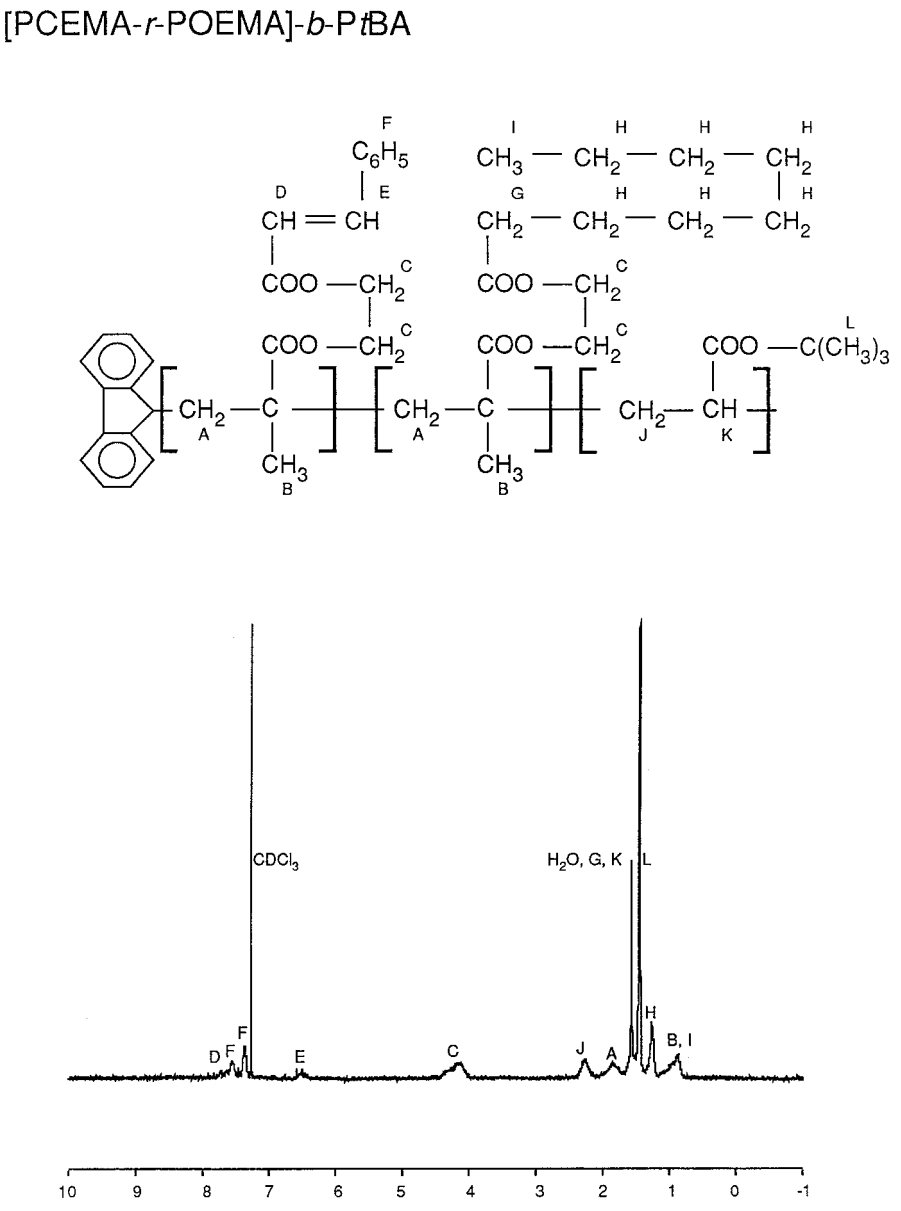

Figure 1 ^{1}H NMR spectrum of a P(CEMA-*ran*-OEMA)-*b*-P*t*BA sample with an OEMA molar fraction of 30% in $CDCl_3$.

take more perylene, regardless how much perylene is present. The majority of the excess perylene will exist as microcrystals in the water, which settle on centrifuge and do not contribute to further fluorescence intensity increase. The settling of perylene microcrystals by centrifugation and that perylene sorbed by nanospheres is responsible for the fluorescence intensity observed can be appreciated from the following observations. After centrifugation to remove perylene particles, the fluorescence intensity of perylene-saturated nanosphere solutions disappeared almost completely with the addition of $CaCl_2$, which precipitated out the nanospheres. The intensity was quantitatively restored with the addition of disodium salt of EDTA, which complexed with Ca^{2+} to redisperse the nanospheres.

Also illustrated in Figure 5 is our method for determining the capacity of the nanospheres. The maximal amount of perylene the nanospheres can uptake is determined to be 0.75 μg from the cross-

Table II Characteristics of the Nanospheres and Micelles Used

Sample	CEMA Conversion	dn_r/dc ($g \cdot g^{-1}$)	$10^{-5}\bar{M}_w$ ($g \cdot mol^{-1}$) from LS	R_G/nm from LS	R_h/nm from LS[a]
Nanosphere 1	15%	0.110	75	34	42 ± 2
Nanosphere 2	20%				55 ± 2
Nanosphere 3	35%				64 ± 2
Nanosphere 4	30%				65 ± 2
PS-*b*-PAA Micelles					41

LS, light scattering.
[a] R_h of the nanospheres were measured in DMSO and that of PS-*b*-PAA micelles was measured in a 0.100*M* aqueous HCl solution. The PS-*b*-PAA micelle R_h value increased to 55 nm when the scattering angle decreased to 45°.

ing point between the straight lines describing intensity-*vs.*-perylene amount data at high and low perylene contents. Because the total amount of nanospheres present was 0.344 mg, the capacity of the nanospheres was 2.2 $mg \cdot g^{-1}$ and the capacity of the nanosphere cores is 3.1 $mg \cdot g^{-1}$ after the core weight fraction of 0.70 was taken into consideration. Capacities of the PS-*b*-PAA micelles and other nanospheres were determined in a similar fashion and the results are compared in Table III.

Factors Affecting Core Capacity

The core capacities are typically ~ 3.5 $mg \cdot g^{-1}$ for our samples. These values are disappointingly low for practical applications. The perylene partition equilibrium can be expressed by

$$P(s) \rightleftharpoons P(w) \overset{K}{\rightleftharpoons} P(N) \quad (1)$$

where P(s), P(w), and P(N) represent solid perylene, perylene in water, and perylene in

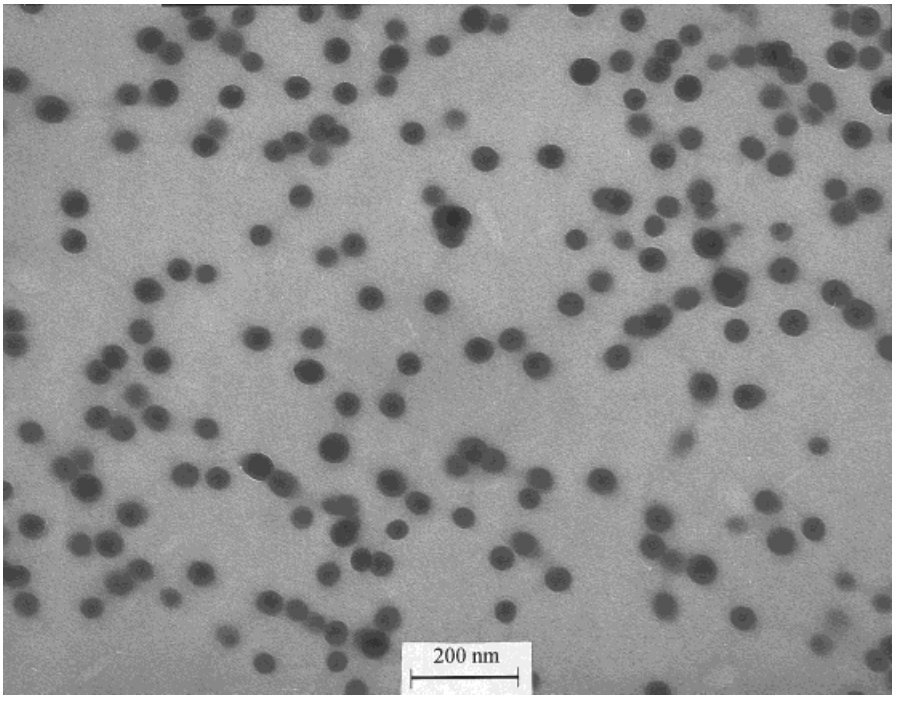

Figure 2 TEM image of nanosphere 4. The TEM specimen was prepared by spraying a dilute nanosphere solution in water onto Formvar-coated copper grids.

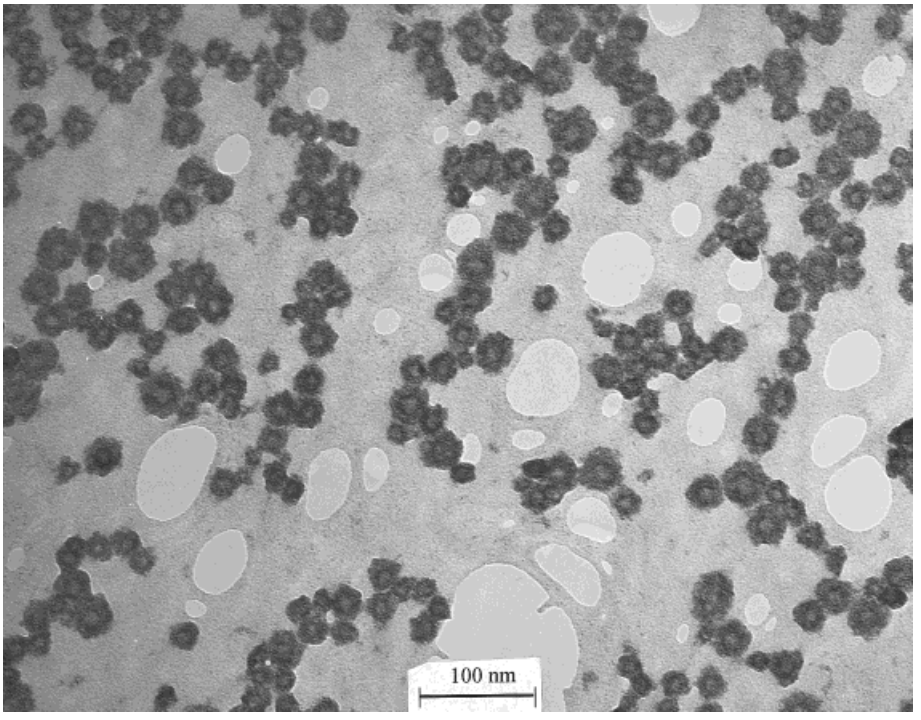

Figure 3 TEM image of PS-*b*-PAA micelles.

nanosphere core, respectively. The perylene partition coefficient K is:

$$K = \frac{\gamma_{P(N)}[P(N)]}{\gamma_{P(w)}[P(w)]} \quad (2)$$

with γ denoting the activity coefficient of each component. If an excess of solid perylene is used, perylene concentration in the aqueous phase should be equal to its solubility. Due to perylene's low solubility in water, $\gamma_{P(w)}$ is close to 1. To increase the nanosphere capacity or the equilibrium perylene concentration in nanosphere cores, $[P(N)]$, one can increase either K or $[P(w)]$ according to eq. (2).

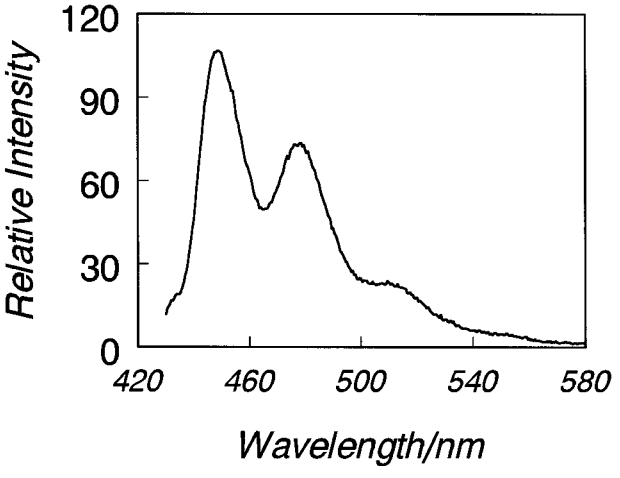

Figure 4 Fluorescence spectrum of perylene in a nanosphere solution at the nanosphere concentration of 2.09×10^{-5} g · mL^{-1}.

Capacities of Different Nanospheres and PS-*b*-PAA Micelles

Capacities of different nanospheres and the PS-*b*-PAA micelles are given in Table III. The core capacities changed from sample to sample. This suggests that changing the core structure can effect K value change and thus the nanosphere capacities. Due to the relatively large errors in the capacity values, further rationalization of the core capacity variation trend would not be warranted.

Significant errors are associated with the capacity values because of the line crossing method used for their determination. The line intersection point shown in Figure 5 depends on how the lines, particularly the line through data for the low perylene amount samples, are drawn. If a straight line is drawn through the initial two data

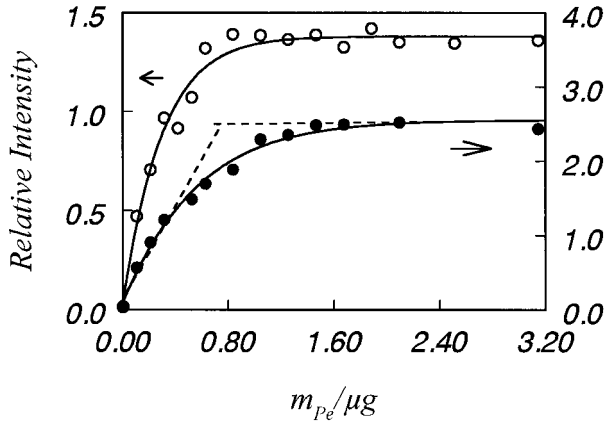

Figure 5 Increase in perylene fluorescence intensity as a function of the amount of perylene added, m_{Pe}, to 4.00 mL of nanosphere 3 (●, 0.086 g · L^{-1}) and PS-*b*-PAA micellar (○, 0.236 g · L^{-1}) solutions.

points, the capacity value would have been significantly lower.

Because the saturation concentration of perylene in water is $2 \times 10^{-9}M$,[16] this concentration and eq. (2) can be used to calculate the perylene partition coefficients. For this, we assumed a core density, ρ_c, of 1.0 g · mL^{-1} and a perylene activity constant, $\gamma_{P(N)}$, of 1 in the nanosphere cores. The perylene equilibrium molar concentration in the cores can be calculated from the capacities, C, using,

$$[P(N)] = \frac{\rho_c C}{M} \tag{3}$$

where M is the molar mass of perylene. The partition coefficients calculated this way are ~ 6×10^6, and the results for different nanospheres and the PS-*b*-PAA micelles are shown in Table III. These values compare well with the coefficient of 3.6×10^6 for perylene partition between polystyrene and water[15] and that of 1.7×10^6 between octanol and water.[17]

Effect of DMSO on Nanosphere Capacities

According to eq. (2), the capacities may increase with hydrocarbon solubilities in water. Our previous studies indicated the nanospheres were able to extract a lot of DMSO from water (i.e., up to 115% of their own volume). This seems to suggest the validity of the hypothesis. We also measured the perylene uptake capacity by the nanospheres in water/DMSO with 1%, by volume, of DMSO. Under otherwise identical conditions, the use of 1% DMSO increased the core capacity of nanosphere 2 to 21.0 mg · g^{-1}, which represents a 5.3-fold increase over that determined when water was used as the solvation medium. The capacity increase may have derived from the higher solubility of perylene in water/DMSO than in pure water.

Validity of the Capacity Data

Concerns may be raised about the validity of our experiments in determining the core capacities. One possible explanation for the leveling off of the fluorescence intensity, in Figure 5, with perylene

Table III Capacities of the Nanospheres and Micelles

Sample	Conc. (g · L^{-1})	Polymer (mass · mg^{-1})	Perylene (mass · μg^{-1})	Capacity (mg · g^{-1})	Core Capacity (mg · g^{-1})	$K \times 10^{-6}$
			In Water			
Nanosphere 2	0.068	0.272	0.77	2.8	4.0	7.9
Nanosphere 3	0.086	0.344	0.75	2.2	3.1	6.1
Nanosphere 4	0.070	0.280	0.77	2.8	3.9	7.3
The Micelles	0.236	0.944	0.31	0.33	2.8	5.5
Capacity in Water: Fluorescence Intensity Measured in Benzene after Perylene Extraction						
Nanosphere 3	0.077	0.308	0.94	3.1	4.4	
			In Water/DMSO (v/v = 99/1)			
Nanosphere 2	0.068	0.272	4.0	14.7	21.0	

amount is that the fluorescence quantum yield of nanosphere-sorbed perylene decreases, due to "concentration quenching," after a critical perylene loading density is reached in the nanosphere cores. After this critical loading density, the amount of perylene sorbed may still increase, the decreasing quantum yield cancels the effect of this increasing perylene loading density, and the fluorescence intensity from the nanosphere-sorbed perylene thus levels off.

The invalidity of the above argument can be appreciated from the following three observations. First, we did not see any excimer formation resulting from concentration quenching from nanosphere-sorbed perylene, regardless of the amount of perylene used in the experiment described in Figure 5. Second, the critical perylene loading density after which concentration quenching occurs should be lower in the perylene-nanosphere solution in water/DMSO due to the increased mobility of perylene in the DMSO-swollen cores. The fact that the perylene uptake capacity of nanosphere 2 in water/DMSO increased relative to the pure water case rules out the possibility, at least for the studies conducted in water, that the leveling off in the perylene fluorescence intensity, shown in Figure 5, at high solid perylene contents was caused by concentration quenching. Third, we measured the core capacity of nanosphere 3 by a different method and obtained a value of 4.4 $mg \cdot g^{-1}$, which is close to 3.1 $mg \cdot g^{-1}$ determined by the standard method. The alternative method differs from the standard method only in that the perylene fluorescence intensity was measured after the perylene was extracted out of the perylene-sorbed nanospheres with benzene. In this way, no concentration quenching is possible, because the perylene concentration in benzene was low.

Precipitation of the Nanospheres or Micelles by Ca^{2+} Addition

Illustrated in Figure 6 are the titration curves of perylene-saturated nanosphere 2 and PS-*b*-PAA micelle solutions by $CaCl_2$. Also shown is that of a perylene-saturated nanosphere 2 solution by KCl. The fact that the perylene fluorescence did not decrease with the addition of 0.100*M* KCl, other than the dilution effect, suggests that neither K^+ nor Cl^- quenched perylene fluorescence. Since K and Ca have similar atomic numbers, Ca^{2+} should not quench the fluorescence significantly either.

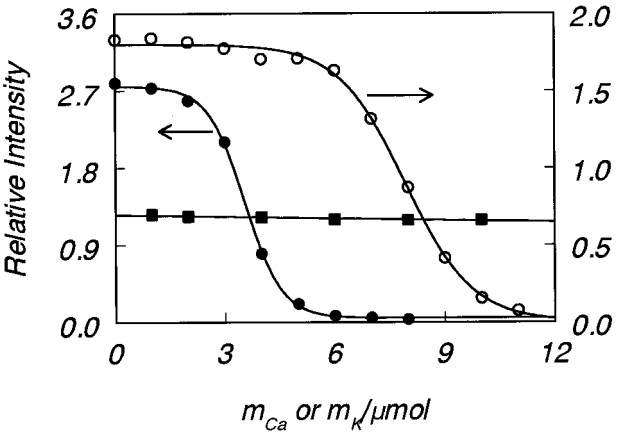

Figure 6 Decrease in the fluorescence intensity of 2.50 mL of perylene-saturated nanosphere 2 (●, 0.068 mg · mL) and PS-*b*-PAA micelle (○, 0.33 mg · mL) solutions with the addition of $CaCl_2$. Also shown (■) is the effect of adding KCl to 2.00 mL of a nanosphere 2 solution at a concentration of 0.034 mg · mL.

The Ca^{2+} cation did not quench the perylene fluorescence. The almost complete disappearance of the perylene fluorescence upon the addition of sufficient Ca^{2+} must have been caused by the precipitation of perylene with the nanospheres. The precipitated nanospheres were actually physically visible.

Because the nanosphere 2 solution was at $c_N = 6.8 \times 10^{-2}$ $mg \cdot mL^{-1}$, the number of mole of AA units in 2.50 mL of solution and the AA molar concentration in this system were 7.1×10^{-7} and 2.84×10^{-4}, respectively, based on data of Table I. The complete precipitation of the nanospheres with trapped perylene at a AA concentration of $2.84 \times 10^{-4}M$ or an estimated nanosphere concentration of $\sim 10^{-9}M$ suggests the tremendous precipitation power of Ca^{2+}. This also explains why PAA nanochannels in thin polymer films prepared by us closed completely by the addition of $CaCl_2$.[18]

The titration endpoint has been defined as the point at which perylene fluorescence intensity decreased by half from its initial value. For nanosphere 2, the endpoint corresponds to the consumption of 3.6 μmol of Ca^{2+}, 5.1 times the molar equivalent of AA, or a Ca^{2+} concentration of $1.44 \times 10^{-3}M$ in 2.50 mL of nanosphere solution.

Shown in Table IV are the titration results for the other nanospheres and micelles. The $[Ca^{2+}]$ at the titration endpoints, $[Ca^{2+}]^*$, were all $\sim 2.0 \times 10^{-3}M$. This sufficiently high Ca^{2+} concentra-

Table IV Ca^{2+} Titration Data for Different Nanospheres and Micelles

Polymer Concentration ($mg \cdot mL^{-1}$)	Polymer Amount (mg)	AA Amount (μmol)	Ca^{2+} Amount (μmol)	10^3 $[Ca^{2+}]$* (M)	$[Ca^{2+}]/[AA]$
		Nanosphere 2			
0.068	0.170	0.71	3.6	1.44	5.1
0.068	0.136	0.57	3.1	1.55	5.4
0.034	0.068	0.284	3.3	1.65	11.6
0.0170	0.034	0.142	3.5	1.75	24.6
		Nanosphere 3			
0.086	0.172	0.72	3.7	1.80	5.1
0.043	0.086	0.36	4.0	2.0	11.1
0.0215	0.043	0.180	4.0	2.0	22.2
		Nanosphere 4			
0.070	0.140	0.58	3.7	1.85	6.3
0.035	0.070	0.292	4.4	2.20	14.9
0.0175	0.035	0.146	4.6	2.30	31
		PS-*b*-PAA Micelles			
0.33	0.83	10.2	7.9	3.2	0.77
0.33	0.66	8.2	6.7	3.3	0.82
0.165	0.33	4.1	7.0	3.5	1.71
0.083	0.165	2.05	5.8	2.9	2.83

tion is advantageous because this would make the nanospheres stable in natural water where some divalent cations are present.

Critical Ca^{2+} Concentration, $[Ca^{2+}]$*, for Nanosphere Precipitation

The $[Ca^{2+}]$* values varied little with nanosphere or micelle concentrations, but are nanosphere-type-dependent. This can be advantageous because one does not need to worry about concentration-dependent nanosphere precipitation and can focus on the design of a particular type of nanospheres for a certain aqueous environment. We do not know exactly how the different structural factors affect $[Ca^{2+}]$*. All the nanosphere samples examined had the same PAA length and the same mass ratio between the PAA and hydrophobic blocks due to the close match between the molar masses of the cinnamoyl and octanoyl groups. Thus, the different sizes of the nanospheres (Table II) must have been responsible for the $[Ca^{2+}]$* change. It seems that $[Ca^{2+}]$* increase with the size of nanospheres.

The invariance in $[Ca^{2+}]$* with nanosphere concentration suggests the following equilibrium:

$$\text{AA-H} + Ca^{2+} \overset{K_{Ca}}{\rightleftharpoons} Ca(AA)^{+} + H^{+} \qquad (4)$$

where K_{Ca} denotes the constant for Ca^{2+} and AA complex formation; AA-H on the left-hand side denotes an AA unit with the carboxyl proton, and the AA on the right-hand denotes an AA unit without the carboxyl proton. At a titration endpoint,

$$K_{Ca} = \frac{[H^+][Ca(AA)^+]}{[AA][Ca^{2+}]^*} \qquad (5)$$

and $[Ca(AA)^+]/[AA]$ should be approximately constant. Because the nanosphere concentration is low, pH of the solution is largely determined by the CO_2 present in water and varies little from sample to sample. A constant K_{Ca} suggests little variation in $[Ca^{2+}]$* with nanosphere concentration.

Redispersion of Precipitated Nanospheres by EDTA

Illustrated in Figure 7 is the comparison between perylene fluorescence spectra before Ca^{2+} addi-

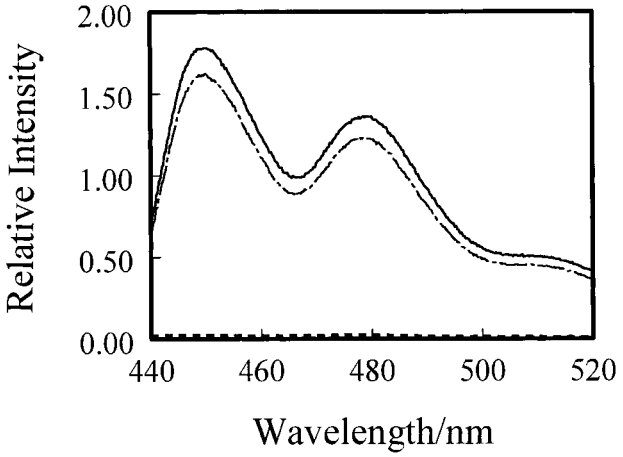

Figure 7 Comparison of the perylene fluorescence spectra of a 2.50 mL perylene-saturated nanosphere 2 solution at $c_N = 6.8 \times 10^{-2}$ mg · mL (——), after the addition of 80 μL of a 0.100*M* $CaCl_2$ solution (- - -) and the addition of 120 μL of a 0.100*M* EDTA solution (– · –). The intensity of the latter two spectra were corrected for the dilution due to the addition of $CaCl_2$ and EDTA solutions.

tion, after Ca^{2+}-induced nanosphere precipitation, and after nanosphere redispersion by the addition of disodium salt of EDTA. To induce precipitation in a 2.50 mL nanosphere 2 solution at $c_N = 6.8 \times 10^{-2}$ mg · mL^{-1}, 80 μL of a 0.100*M* $CaCl_2$ solution was used. To redisperse the nanospheres, we injected 120 μL of a 0.100*M* EDTA solution. After such a cycle, perylene fluorescence intensity was completely recovered within experimental error. This again points to the fact that calcium in the Ca(EDTA) form did not quench perylene fluorescence.

The complete signal disappearance and then recovery suggests that perylene always stayed with the nanospheres. Also, it is possible to insert a step between the nanosphere precipitation and redispersion so that one can extract the PAHs out of the nanospheres using an organic solvent. After the removal of the trapped PAHs, the nanospheres can be reused by dispersion with EDTA or better with CO_3^{2-}, which precipitate Ca^{2+}.

Comparison of Rates of Perylene Insertion into Different Cores

The insertion of perylene from the aqueous phase into the core of a nanosphere increases its fluorescence quantum yield. Illustrated in Figure 8 is the increase in perylene fluorescence intensity as a function time after the aqueous perylene solution was mixed with a nanosphere 1 solution. We fitted the data of perylene fluorescence intensity increase with time t using:

$$I(t) = a_0 - a_1 \exp(-t/\tau_1) - a_2 \exp(-t/\tau_2) \quad (6)$$

The perylene entrance rate was then characterized by $1/\langle\tau\rangle$ with

$$\langle\tau\rangle = \frac{a_1\tau_1 + a_2\tau_2}{a_1 + a_2} \quad (7)$$

Table V summarizes the $\langle\tau\rangle$ values determined for the nanospheres and PS-*b*-PAA micelles. The kinetics was performed all at equal hydrophobic core mass concentrations. The typical $\langle\tau\rangle$ is $\sim 2 \times 10^4$ s or 5.5 h.

The first feature is that the rate of perylene insertion into nanosphere 3 increased with a decrease in CEMA crosslinking density from 35% to 0%. This rate increase was, however, not substantial. The second feature was rather surprising. The incorporation of OEMA into the core was expected to increase the rate of perylene diffusion, because POEMA should be a rubbery polymer instead of a

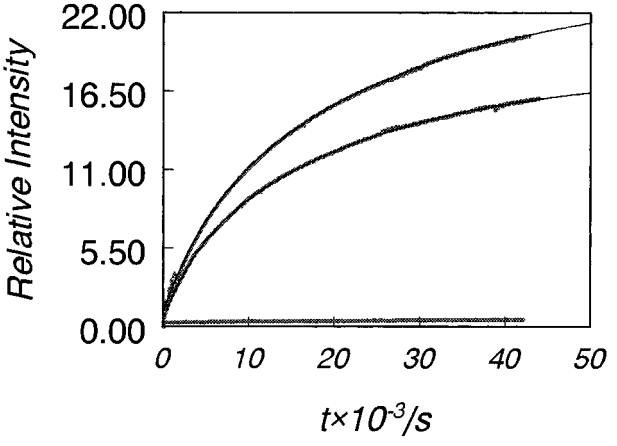

Figure 8 Under identical instrumental settings and equal perylene concentrations, the fluorescence intensity of a perylene solution in water did not increase significantly with continuous irradiation by the excitation source (bottom). The fluorescence intensity of perylene increased after the addition of either the nanosphere (top) or the micelle (middle) sample. The final nanosphere and micelle concentrations after sample mixing were 5.6×10^{-5} and 26.8×10^{-5} g · mL^{-1}, respectively. The solid curves represent the best fit to experimental data by eq. (6).

Table V Parameters Generated from Fitting Kinetic Data of Perylene Uptake by Nanospheres

Sample	c_N/mg · mL^{-1}	CEMA Conversion	τ_1/s	τ_2/s	$\frac{\langle\tau\rangle}{s}$	R_{val}
Nanosphere 1	5.6×10^{-2}	15%	3.6×10^3	2.20×10^4	1.81×10^4	1.000
Nanosphere 2	5.6×10^{-2}	20%	6.8×10^3	3.67×10^4	2.59×10^4	0.998
Nanosphere 3	5.6×10^{-2}	35%	5.2×10^3	2.74×10^4	2.21×10^4	1.000
Nanosphere 4	5.6×10^{-2}	30%	1.28×10^3	3.07×10^4	2.53×10^4	1.000
Micelles of polymer 3	5.6×10^{-2}	0%	2.31×10^3	2.23×10^4	1.59×10^4	0.999
PS-*b*-PAA micelles	26.8×10^{-2}	0%	1.97×10^3	2.97×10^4	2.41×10^4	1.000

glassy polymer like PCEMA. In reality, $1/\langle\tau\rangle$ of nanosphere 4 did not increase over that of nanosphere 2. One possible reason is that the molar concentration of nanosphere 4 was substantially lower than that of nanosphere 2 at an equal mass concentration, because nanosphere 4 was larger than nanosphere 2, as judged from their R_h values (Table V). The other possible reason is that the dissociation of colloidal perylene into molecular perylene is the rate-determining step for perylene insertion.

CONCLUSIONS

PCEMA-*b*-PAA and P(CEMA-*ran*-OEMA)-*b*-PAA nanospheres were prepared. Also prepared were PS-*b*-PAA micelles. All of these nanospheres and micelles uptook perylene with similar rates, partition coefficients, and core capacities. They were all precipitated by $CaCl_2$. These results suggest that one can safely replace some of the CEMA units of the PCEMA block with OEMA to eliminate the potential problems caused by the further crosslinking of the PCEMA cores in sunlight. Detailed analysis indicated that the capacity of the cores in uptaking a PAH is governed mainly by two factors: the structure of the core that determines the magnitude of the partition coefficient and solubility of PAH in the aqueous medium. The calcium concentration for nanosphere precipitation is independent of the nanosphere concentration, but are nanosphere-type-dependent.

The authors wish to acknowledge the Research Grant Program of NSERC and the University of Calgary for financial support of this research. Dr. Jianfu Ding is gratefully acknowledged for obtaining the TEM images.

REFERENCES

1. (a) Z. Tuzar, in *Solvents and Self-Organization of Polymers,* Kluwer Academic Publishers, Dordrecht, The Netherlands, 1996; (b) R. Nagarajan, in *Solvents and Self-Organization of Polymers,* Kluwer Academic Publishers, Dordrecht, The Netherlands, 1966.
2. (a) L. Zhang and A. Eisenberg, *Science,* **268,** 1728 (1995); (b) H. Shen, L. Zhang, and A. Eisenberg, *J. Phys. Chem. B,* **101,** 4697 (1997).
3. W.-Y. Chen, P. Alexandridis, C.-K. Su, C. S. Patrickios, W. R. Hertler, and T. A. Hatton, *Macromolecules,* **28,** 8604 (1995).
4. P. Alexandridis, U. Olsson, and B. Lindman, *Macromolecules,* **28,** 7700 (1995).
5. B. Chu, *Langmuir,* **11,** 414 (1995).
6. A. Qin, M. Tian, C. Ramireddy, S. E. Webber, P. Munk, and Z. Tuzar, *Macromolecules,* **27,** 120 (1994).
7. M. Ikemi, N. Odagiri, S. Tanaka, I. Shinohara, and A. Chiba, *Macromolecules,* **14,** 34 (1981).
8. R. Xu, M. A. Winnik, G. Riess, B. Chu, and M.-D. Croucher, *Macromolecules,* **25,** 644 (1992).
9. F. Henselwood and G. Liu, *Macromolecules,* **30,** 488 (1997).
10. G. Wang, F. Henselwood, and G. Liu, *Langmuir,* **14,** 1554 (1998).
11. G. Liu, J. Ding, A. Guo, M. Herfort, and D. Bazett-Jones, *Macromolecules,* **30,** 1851 (1997).
12. (a) M. E. Jung and M. A. Lyster, *J. Am. Chem. Soc.,* **99,** 968 (1976); (b) G. A. Olah and S. C. Narang, *Tetrahedron,* **38,** 2225 (1982).
13. C. K. Smith and G. Liu, *Macromolecules,* **29,** 2060 (1996).
14. J. Ding and G. Liu, *Macromolecules,* **30,** 655 (1997).
15. M. Nowakowska, B. White, and J. E. Guillet, *Macromolecules,* **22,** 2317 (1989).
16. R. Pearlman and S. H. Yalkowsky, *J. Phys. Chem. Ref. Data,* **13,** 555 (1984).
17. H. Gusten, D. Horvatic, and A. Sabljic, *Chemosphere,* **23,** 199 (1991).
18. J. Ding and G. Liu, *Adv. Mater.,* **10,** 69 (1998).